Computational and Structural Biotechnology Journal 20 (2022) 5440–5452

COMPUTATIONAL ANDSTRUCTURAL BIOTECHNOLOGY JOURNAL

journal homepage: www.elsevier.com/locate/csbj

Pyroptosis-related gene expression patterns and corresponding tumor microenvironment infiltration characterization in ovarian cancer

Jinhui Liu [a,1], Can Chen [b,1], Rui Geng [c,1], Fang Shao [c,1], Sheng Yang [c], Zihang Zhong [c], Senmiao Ni [c], Jianling Bai [c,*]

[a] Department of Gynecology, The First Affiliated Hospital of Nanjing Medical University, Nanjing 210029, Jiangsu, China
[b] Department of Laboratory Medicine, The First Affiliated Hospital of Nanjing Medical University, 300 Guang Zhou Road, Nanjing 210029, Jiangsu Province, China
[c] Department of Biostatistics, School of Public Heath, Nanjing Medical University, 101 Longmian Avenue, Jiangning District, Nanjing 211166, China

ARTICLE INFO

Article history:
Received 18 April 2022
Received in revised form 6 September 2022
Accepted 26 September 2022
Available online 28 September 2022

Keywords:
Pyroptosis
TCGA
Ovarian cancer
Tumor immune environment
Immune checkpoint inhibitors

ABSTRACT

Pyroptosis, a form of inflammatory programmed cell death, is accompanied by inflammation and participate in the body's immune response. The expression of pyroptosis-related genes (PRGs) is associated with tumor prognosis in ovarian cancer (OC), but it is still unknown whether pyroptosis can affect tumor immune microenvironment (TME) of OC. Based on 30 PRGs, we comprehensively assessed the pyroptosis patterns by using PRGscore and correlated them with TME features in 474 OC patients. Finally, we identified three pyroptosis modification patterns and TME immune characteristics of these patterns were in response to three immune phenotypes (immune-desert, immune-inflamed, and immune-excluded phenotypes). PRGscore can predict patient survival, staging, grading, and immunotherapy efficacy. Low PRGscore was associated with better survival advantage and increased mutation burden. Low PRGscore patients showed significantly better therapeutic effects and clinical results in chemotherapy and immunotherapy. Besides, the capability of PRGscore in predicting prognosis and immunotherapy sensitivity was further verified in other three tumor cohorts. In conclusion, the comprehensive assessment of OC pyroptosis modifications can help enhancing our understanding of TME immune infiltration and provide better personalized treatment tactics for OC patients.

1. Introduction

OC is a tumor that grows on the ovary. Its incidence is relatively high, ranking third after cervical cancer and endometrial carcinoma [1]. Approximately 70 % of patients are at a late stage at diagnosis, and treatment for late OC is poor [2,3]. The standard treatment protocol for OC is surgery, supplemented by a combination of platinum and paclitaxel drugs [4,5]. However, the therapeutic effect is not optimistic, and approximate 25 % to 30 % of patients developed drug resistance [6,7].

Immune checkpoint inhibitors (ICIs), have shown superiority of treatment effect over conventional therapies in many tumors, particularly in lung cancer, melanoma and kidney cancer, which dramatically improv overall survival for patients [8,9]. For example, a study found a significant trend towards longer objective remission rates (ORR) and overall survival in recurrent OC patients receiving pembrolizumab (*PD-1* inhibitor) monotherapy[10]. Nivolumab (*PD-1* inhibitor) was effective and safe in the remedy of patients with recurrent platinum-resistant OC. However, there was a dose-dependent response of 20 %–33 % when treated with nivolumab individually or coupled with anti-CTLA-4 antibody [11]. However, there are still many patients who may not respond to ICI or are resistant to it [12]. Tumor's own immune profile largely influences the immunological efficacy of the patient's treatment [13,14]. Full understanding of TIME infiltration is of clinical significance in predicting whether a patient will benefit from immunotherapy [15].

Pyroptosis, a kind of cellular inflammatory necrosis, refers to the activation of a variety of caspases mediated by inflammasomes, which results in shearing and multimerization of various Gasdermin family members, leading to cell perforation and thus to programmed cell death [16,17]. Compared with apoptosis, pyroptosis occurs more rapidly and is followed with the releasing of many pro-inflammatory factors [18,19]. When pyroptosis occurs, the cell swells and a protrusion forms on the cell before it ruptures, after which pores form in the cell membrane, leading

* Corresponding author.
E-mail address: baijianling@njmu.edu.cn (J. Bai).
[1] Jinhui Liu, Can Chen, Rui Geng and Fang Shao contributed equally to this work.

https://doi.org/10.1016/j.csbj.2022.09.037

to the loss of integrity and releasing of the contents, and triggering an inflammatory reaction [20]. The pyroptosis signaling pathway can be divided into 2 categories: caspase-1-mediated classical pathway and caspase-4, 5, and 11- mediated non-classical pathway [17,21]. Among them, the classical pathway refers to the activation of caspase-1 by intracellular pattern recognition receptors (PRRs). On one side, activated caspase-1 cleaves Gasdermin D (*GSDMD*) and creates a peptide which contains the nitrogen-terminal active structural region of *GSDMD*, which induces cytosolic perforation, cell rupture, content release and an inflammatory response; alternatively, activated caspase-1 cleaves *IL-1β* and *IL-18* precursors and produces active *IL-1β* and *IL-18*, which are released extracellularly leading to the accumulation of inflammatory cells and amplification of inflammation [21]. Differently, the non-classical pathway initiates pyroptosis by activating caspase-4, 5 and 11 to cleave *GSDMD* [17]. Inflammasomes, Gasdermin protein family and pro-inflammatory cytokines are the key effector molecules of pyroptosis [22]. The inflammasome is a multiprotein signal transduction complex [23]. When a host-derived or pathogen-derived danger signal is detected, the inflammasome will begin to assemble in the cytoplasm to promote the release of cytokines and the pyroptotic cell death and inflammation [24]. GSDM family contains *GSDMA, GSDMB, GSDMC, GSDMD, GSDME* and *DFNB59* [25]. In tumor cells, *GSDMC* can convert the process of apoptosis into pyroptosis and promote tumor necrosis [26]. Danger signals released in tumor infiltrating macrophages and dendritic cells can also activate GSDMD-mediated pyroptosis of tumor infiltrating lymphocytes (TILs), thereby enhancing antigen presentation and functional activity [27]. These confirm that pyroptosis is critical in tumorigenesis and progression.

Given the available research results, we know that pyroptosis has a major function in the development of OC and in the antitumor process [28]. However, there are few studies on the specific functions of pyroptosis in TIME and immunotherapy of OC. Therefore, we calculated the modification patterns of pyroptosis death and immune features in OC in an integrated manner and linked the modification patterns of pyroptosis to immune features. We defined three different pyroptosis modification modes and found that they have different immune characteristics, which indicates that pyroptosis modification is critical in shaping the immune landscape of individual OC. In addition, a score was established according to the characteristics of pyroptosis-related genes (PRGs) to quantitate individual OC patient's pyroptosis modification patterns. The scoring system can assist clinicians in formulating efficient and personalized immunotherapy strategies.

2. Materials and methods

2.1. Ovarian cancer dataset source and processing

Fig S1 shows the research process of this article. Public RNA-seq data and full clinical data were searched in the Cancer Genome Atlas (TCGA) [29], Genotype-Tissue Expression (GTEx, version 7) [30], and Gene-Expression Omnibus (GEO) [31]. Gene expression information and corresponding clinicopathological data were downloaded from TCGA database and gene transcriptome data were obtained from GTEx database for normal human ovarian tissue [32]. Because of the missing of normal tumor in TCGA-OC dataset, we treated the gene expression in GTEx as the normal group, and applied the R package *limma* and *sva* to remove the batch effect between the TCGA and GETx datasets and define the PRGs [33,34]. Totally, we obtained 88 normal tissues and 379 tumor tissues. Considering the similarity of clinical information between GSE9891 (285 OC patients) and TCGA-OC, we removed the batch effect using the R package *sva* and merged the clinical information. Then, copy number variation (CNV) from TCGA-OC was downloaded for CNV analysis. Somatic mutation data were utilized to compute the tumor mutational burden (TMB). R (version 4.1.0) was utilized to process and analyze the data.

2.2. Selection and differential expression analysis of PRGs

We extracted 33 PRGs from prior reviews(Table S1) [28]. We then used the limma package to assess the difference in PRGs expression between OC and non-cancerous samples. Subsequently, heat maps and violin graphs were created to show the expression of the differentially expressed PRGs between the two groups. Heat maps of variant genes were created using the 'pheatmap' package [35].

2.3. Data collection of somatic variants

Considering the potential of TMB in forecasting the response to immunotherapy, we carried out a stratified survival analysis that evaluated the connection between TMB and PRGs score. The maftools package [36] was utilized to profile mutations in PRGs score group and TCGA cohort. We selected top 20 genes that had the highest probability to be mutated.

2.4. Unsupervised clustering for PRGs

After merging TCGA and GSE9891 datasets, we acquired 30 PRGs. First, unsupervised cluster analysis was conducted using ConsensuClusterPlus package to identify PRG patterns among samples according to the expression of 30 PRGs [37]. The samples were divided into clusters with distinct biological features with a consensus clustering algorithm. The parameters were set as "clusterAlg="km", distance="euclidean", reps = 50, pItem = 0.8, pFeature = 1, maxK = 9" while conducting the "ConsensuClusterPlus" package. We fixed the number of resamples to 1000 for robustness of clustering.

2.5. Gene set variation analysis (GSVA) and functional annotation

For the purpose of exploring the biological functions between the groups defined by the expression patterns of the PRGs model, we ran a GSVA enrichment analysis with the GSVA package. GSVA is an unsupervised methodology for assessing variability in pathways and biological processes based on non-parametric assumptions [38]. The "c2.cp.kegg.v6.2.-symbol" gene set obtained from MSigDB database was utilized to run GSVA analysis. The clusterProfiler package was employed to functionally annotate pyroptosis genes with a false discovery rate (FDR) cut-off of < 0.05 [39].

2.6. Immune cell infiltration estimation by ssGSEA

We used the ssGSEA algorithm to calculate the relative abundance per cell infiltration [40]. Gene sets labeling each TME-infiltrating immune cell category were gained from the study, in which multiple human immune cell subtypes were archived. The enrichment fraction computed by ssGSEA analysis was applied to express the relative abundance of TME-infiltrated cells in individual sample.

2.7. Selection of differentially expressed genes (DEGs) between PRGs distinct subtypes

We categorized patients into three different PRG patterns according to expression of 30 PRGs. The limma package was used to identify the DEGs between different modification modes [33].

The criterion for identifying a significant DEG was set at an adjusted P-value < 0.001.

2.8. Construction of PRGscore

To measure PRGs expression patterns for each sample, we proposed a score, referred to PRGscore, to predict the recurrence of OC. DEGs obtained from various PRGs clusters were normalized and overlapping genes were selected. Unsupervised clustering methods were applied to analyze overlapping DEGs and to cluster patients into subgroups for more in-depth analysis. Consensus clustering algorithms were used to delineate how many gene clusters there were and their stability. We then carried out a prognostic analysis for every gene in the trait using a univariate Cox regression model. Genes with a remarkable prediction were retrieved for later analysis. We used principal component analysis (PCA) to build PRGs signature, termed as PRGscore [41].

$$PRGscore = PC1 + PC2 + \cdots + PCp$$

where p is the number of PRGs.

2.9. Quantifying predictors of immune response

Immunophenoscore (IPS) is a determinant of response to anti-CTLA-4 (PD-1) agents and serves to quantify the immunogenicity of tumors [42] which was derived from The Cancer Immunome Atlas (TCIA). ESTIMATE algorithm estimates stromal and immune cells in tumors and infers tumor purity [43]. Tumor tissue with rich immune cell infiltration represents a high level of immune score and a low level of tumor purity.

2.10. Prediction of chemotherapeutic response

For examining the association between PRGscore and response to chemotherapy, we used two first-line chemotherapeutics. Publicly available pharmacogenomic database Cancer Drug Sensitivity Genomics (GDSC) was used to forecast the response of selected drugs to chemotherapy for each OC patient [44]. The half maximum inhibitory concentration (IC50) for patients with OC in different scoring groups was estimated by using pRRophetic package [45].

2.11. Verify the performance of PRGscore in predicting patient responsiveness to ICIs

Further validation of the relationship between PRGscore and immunotherapy efficacy was conducted in a relatively complete anti-PD1/PD-L1 treatment cohort (imvigor210) which could be acquired through the R package "IMvigor210CoreBiologies" [46]. The clinical information of the cohort is shown in Table S2. Samples that lacked validity data were removed, and 298 samples were eventually enrolled. The information of TCGA-UCEC and TCGA-CESC could be downloaded from the online website (https://portal.gdc.cancer.gov/).

2.12. Statistical analyses

Kruskal-Wallis test was utilized to compare the gene expression between groups, and Wilcoxon test was applied for two group comparisons. Kaplan-Meier plotters were applied to plot survival curves. The log-rank test was applied to assess statistical differences of TMB between groups. Survcutpoint method stratified the sample into high and low scoring groups, according to the median risk score. A chi-square test was applied to test the relationship between PRGscore and clinical features. We used Spearman correlation coefficients to estimate the correlation between immune cells and PRGs scores. The CNV landscape of PRG in chromosomes was mapped by using the RCirco package [47]. All statistical p value were two side, with $p < 0.05$ indicating a difference of statistical significance.

3. Result

3.1. Landscape of somatic gene mutation and PRGs expression of in OC

We first analyzed the expression patterns of 33 PRGs between 379 OC (TCGA-OC dataset) and 88 normal tissues (GTEx dataset) between GTEx and TCGA-OC individuals. Interestingly, the expression of majority of PRGs, such as *CASP5*, *CASP9*, *GSDMB* and *GSDMD*, etc. were markedly decreased in OC patients. Conversely, several PRGs including *AIM2*, *CASP3*, *CASP6* and *GSDMA* etc. was significantly higher expressed in OC patients (Fig. 1a). There were two types of pyroptosis: canonical and non-canonical pyroptosis. The core genes in canonical pathway include *NLRP1*, *NLRP3*, *NLRC4*, *AIM2*, *CASP1*, *GSDMD*, and *PYCARD*, and those in non-canonical pathway include *GSDME*, *CASP3*, *CASP4*, *CASP5*, *CASP11*, *CASP8*, *TNF*, *GSDMC*, *GZMB*, *GSDMB*, and *GZMA*. The expression differences of these core genes between patients and controls were specifically presented in Fig S2, showing that most of these core genes were downregulated in tumor tissues compared to those in normal tissues. On the other hand, using log-rank test, we found most of them were protective and adverse prognostic factors, such as *NLRP2* and *TIRAP* ($P < 0.001$, Fig S3). Furthermore, Correlation heatmap was used to elucidate the relevance of the 33 PRGs to each other and showed that *NLRP3* and *PLCG1* may be hub genes of PRGs (Fig. 1b). Interestingly, *NLRP3* was positively correlated with 24 genes, and its expression was highly positively correlated with *NLRC4*, *IL1B*, *CASP1* and others. While *PLCG1* were negatively related with 14 genes, especially *CASP1*, *PYCARD* and *IL18* (Fig. 1b). The expressions of *NLRP3* and *PLCG1* were significantly increased and decreased in OC patients, respectively (Fig. 1a), implying that these might be critical genes in the PRGs that affects tumorigenesis and development.

Furthermore, we concluded the occurrence of CNV in 33 PRGs. Fig. 1c showed widespread CNV alterations in 33 PRGs were mostly copy number deletions, while *GSDMC*, *GSDMD*, *PRKACA* and *NLRP3* had extensive CNV amplification frequencies. The position of the altered CNV of PRGs on chromosome was illustrated in Fig. 1d. According to expressions of 33 PRGs, we fully differentiated between OC and normal tissue (Fig. 1e). With the aim of testing the association between above genetic variants and linked to PRG expression in OC patients, we examined PRG expression levels and observed that CNV alterations may be a major factor in the perturbation of PRGs expression. Expressions of CNV-deficient PRGs were markedly lower in tumor tissues (e.g. *ELANE* and *CASP9*) compared to normal tissues and the opposite was also true (e.g. *GSDMC* and *NLRP3*) (Fig. 1a, c). The above analysis displayed considerable heterogeneity in the genetics and expressions of PRGs between normal and OC tissues, demonstrating that PRGs expression levels may be linked to the onset and progression of OC.

3.2. Immune characteristics in distinct PRGs patterns

After integrating TCGA-OC and GSE9891 datasets, we characterized patients with a PRG expression pattern according to the expression of 30 PRGs and ultimately defined three PRclusters by using unsupervised clustering, with 259 patients included in pattern A, 263 patients in pattern B and 139 patients in pattern C (Fig. 2a and Fig. S4a-b). After that, we grouped samples in GTEx into pattern D. The K-M curve indicated a particular survival disadvantage in PRcluster B pattern ($P = 0.035$, Fig. 2b). Moreover, we

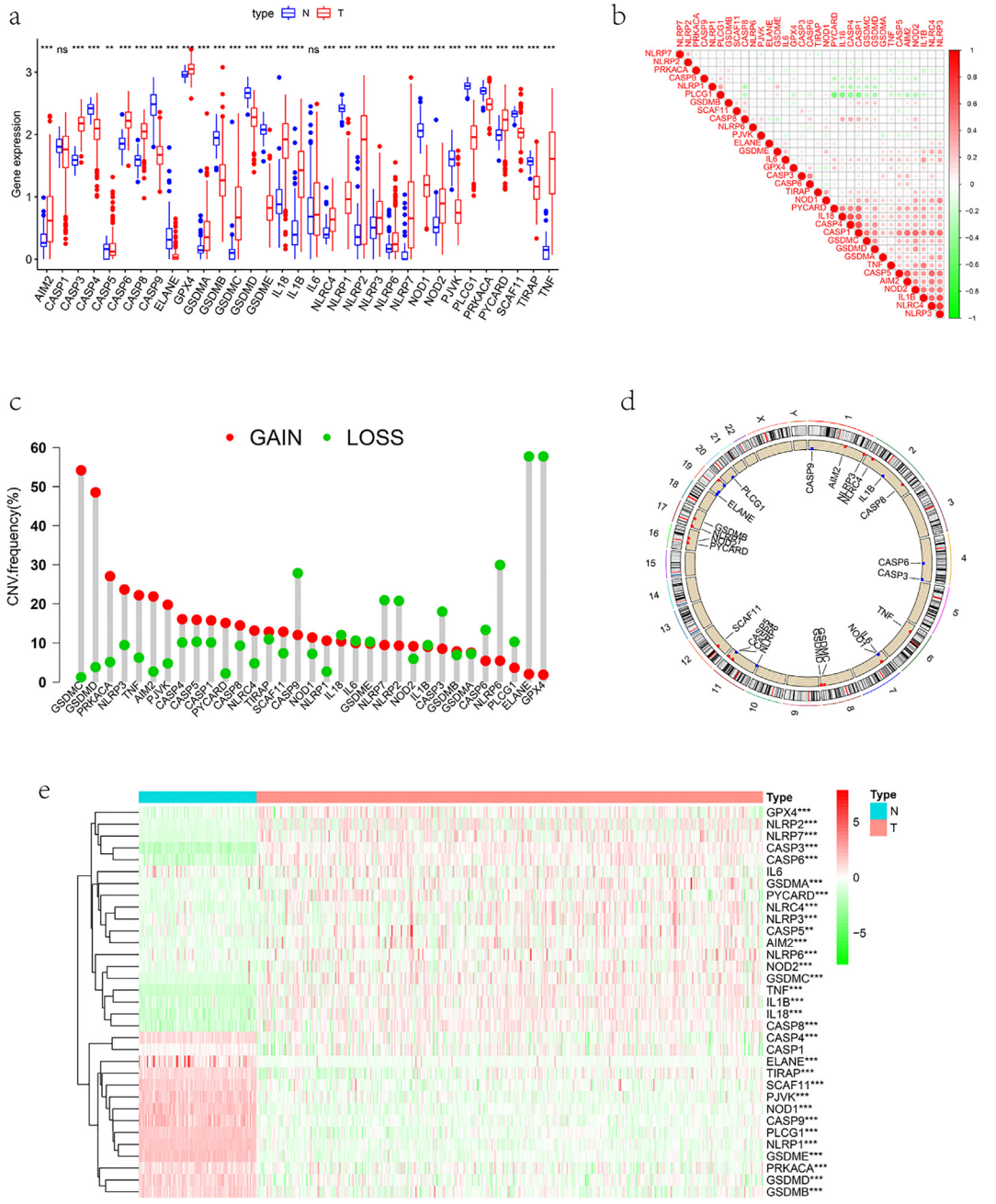

Fig. 1. Landscape of genetic and expression variation of pyroptosis genes in ovarian cancera Differential expression heatmap of pyroptosis genes in OC and normal tissues from TCGA. Tumor, red; Normal, blue. The upper and lower ends of the boxes represented interquartile range of values (*$P < 0.05$; **$P < 0.01$; ***$P < 0.001$). b Connection heatmap of 33 PRGs. c The CNV variation frequency of pyroptosis regulators. d The location of CNV alteration of pyroptosis regulators on 23 chromosomes using TCGA cohort. e Boxplot of pyroptosis genes expression in OC and normal samples. (For interpretation of the references to colour in this figure legend, the reader is referred to the web version of this article.)

ran GSVA enrichment analysis to discover the differences between PRclusters in terms of all gene expression levels. PRcluster-A was heavily enriched in pathways related to immune activation, such as the activation of cytokine–cytokine receptor, interaction and chemokine signaling pathway, TCR signaling pathway and BCR signaling pathway. At the same time, PRcluster-C displayed a rich set of matrix-activated pathways, like cell adhesion and Jak Stat signaling pathways. In contrast, PRcluster-B was strongly involved in the biological process of immunosuppression (Fig. 2c). As healthy control, the biological processes which PRcluster-D mainly involved were obviously different with other clusters (Fig S5). As expect, subsequent result of TME cell infiltration indicated the rank of immune cell infiltration of three cluster was PRcluster-C, PRcluster-A and PRcluster-B (Fig. 2d). The rank of rich was consistent to the survival time of three PRclusters (Fig. 2b and 2d). Moreover, we used the ESTIMATE algorithm to measure immune cell infiltration and tumor purity in three PRG patterns, and studied the biological functions of three clusters in immunological terms. First, PRcluster-C showed the highest immune and stromal scores, followed by PRcluster-A, B (Fig. 2e, f, g), demonstrating the lowest tumor purity in cluster C.

Considering that immune checkpoints can serve as biomarkers for predicting treatment response to ICIs, we compared *PD-L1*, *PD-L2* and *CTLA4* expression levels in different PRGs clusters and

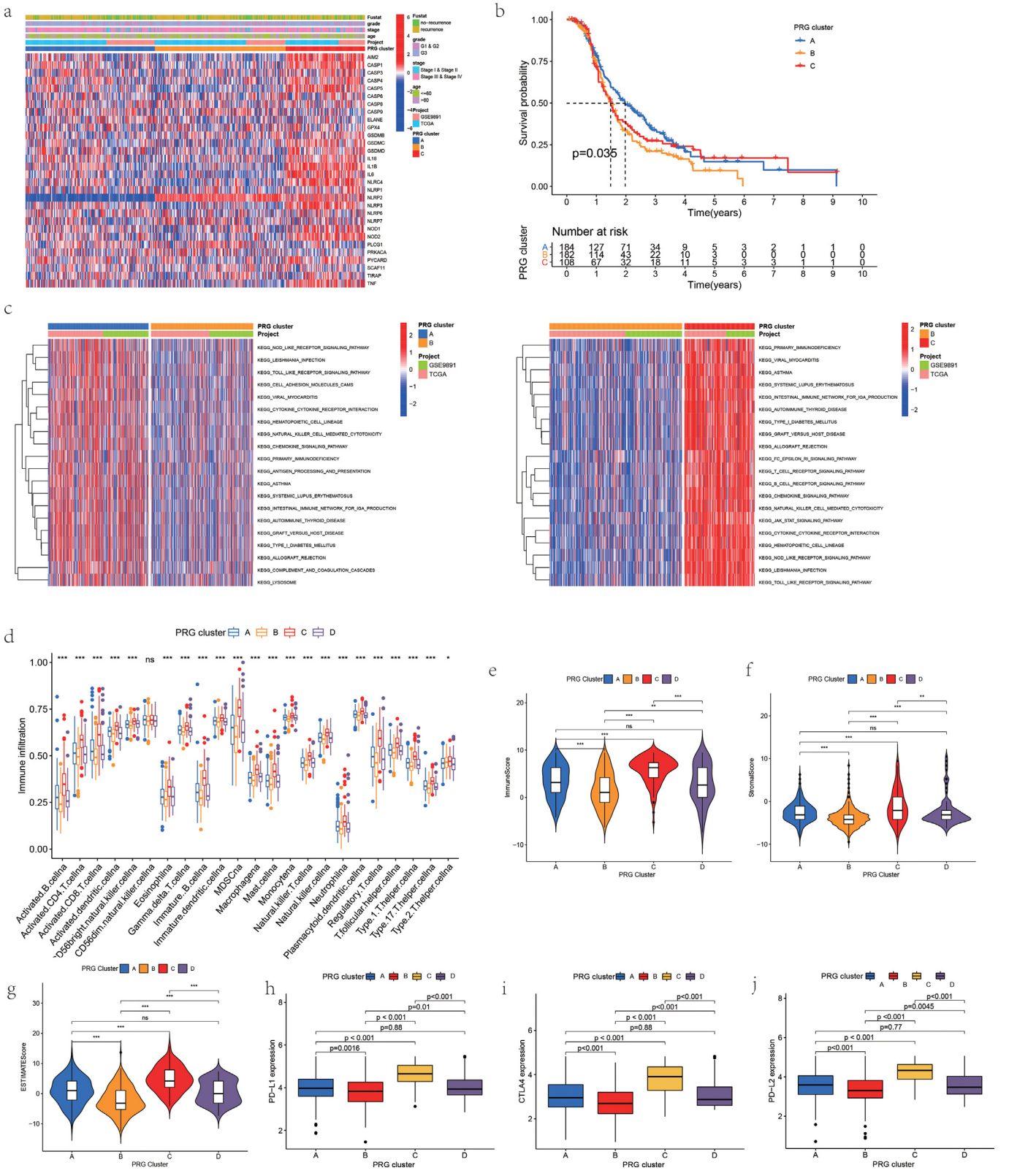

Fig. 2. Pyroptosis modification patterns in OC and biological and immune characteristics of pyroptosis subtypesa Differences in clinicopathologic features and expression levels of PRGs between the three PRGs clusters. b Survival analyses for the pyroptosis clusters, including 184 cases in PRcluster-A, 182 cases in PRcluster-B, and 108 cases in PRcluster-C. c GSVA enrichment analysis indicating the activation states of biological pathways in distinct pyroptosis clusters. The heatmap was applied to visualize these biological pathways. d The abundance of each TME infiltrating cell in three pyroptosis modification patterns. The box plot indicated the difference of immune score(e),stromal score(f) and estimate score (g) between pyroptosis modification patterns. Difference of PD-L1(h),CTLA-4(i) and PD-L2(j) expression among distinct pyroptosis clusters. (Kruskal-Wallis test).

observed a markable expression increase in these genes in cluster-C (Fig. 2h, i, j). We proved that the three PRGs patterns had varied immune infiltration characteristics. In addition, we further explored the characteristics of these PRGs subtypes in different clinical information. At the same time, the immune cell infiltration, TME score and immune checkpoints expression of health control were significantly different from the three PRGs patterns. Similar to the previous study, the tumor staging and cancer recurrence rate of cluster B samples were higher than those in other two clusters (Fig. S4c).

3.3. Generation of PRGs gene clusters and functional annotation

For the purpose of exploring the underlying biological behavior of individual PRGs patterns, we selected 1,024 DEGs using limma package (Fig. 3a). Univariate Cox regression analysis was performed to assess the prognosis of DEGs linked to PRGs subtypes. The biological processes obtained from GO and KEGG enrichment were summarized in Fig. S4d. Amazingly, these genes exhibited substantial enrichment for biological processes related to immunity, reaffirming that PRGs played a non-negligible role in TME immune regulation. 67 PRGs phenotype-related genes with significant prognosis were isolated and used to further characterize PRGs gene signature. We then carried out an unsupervised cluster analysis of 67 genes to categorize patients into four subtypes (Fig. S4e). Patients in gene cluster B have the worst prognostic results (Fig. 3b and S3f). PRGs were remarkably differentially expressed across the four PRGs gene clusters. Generally speaking, the expression profiles of PRGs were the highest in gene cluster C, while the lowest in gene cluster D(Fig. 3c).

Similarly, we applied the ssGESA method to evaluate the immune infiltration in the four gene clusters. The results showed that there were differences in the immune infiltration conditions between the four clusters. The rich levels of immune cell infiltration were gene cluster-C, B, A and D (Fig. 3d). ESTIMATE algorithm results showed that gene cluster C contained the most immune and stromal cells, that is, the lowest tumor purity, followed by gene cluster B, A and D (Fig. 3e). This was consistent with the difference in immune cell infiltration. Moreover, we compared four immune checkpoints expression levels in different gene clusters, and observed that these genes expression levels in gene cluster subtypes were also C, B, A, and D (Fig. 3f). From the above analysis, we confirmed that the four gene clusters did have different immune infiltration characteristics.

3.4. Construction of PRGscore and its TME features and biological processes

Given the individual heterogeneity of PRGs, according to 67 DEGs expression, a scoring model was built to quantitate the PRGs for each OC patient. Alluvial plots are applied to monitor changes in the attributes of single patients (Fig. 4a). Kruskal-Wallis test revealed marked discrepancies in PRGs scores between PRGs clusters and gene clusters (Fig. 4b). More importantly, PRGs cluster B displayed dramatically higher PRGs scores, in contrast to PRGs cluster C, implying that low PRGscore would be strongly correlated with immune activation-related features, while high PRGscore may be correlated with stromal activation-related signatures. Moreover, PRGs gene cluster D showed a significant increase in PRGscores in relation to the other clusters and PRGs gene cluster C showed the lowest score. These results highly emphasized that low PRGscores were clearly linked to immune activation, while high PRGscores were linked to stromal activation. PRGscore allowed a better assessment of pyroptosis pattern of single tumors and better characterization of TME cellular infiltration.

Subsequently, a discussion of the PRG scores of OC patients was conducted to determine their prognostic value. Patients were categorized into high or low PRGscore groups and best cut-off value was identified by log-rank test. Patients with high PRGs scores demonstrated poor outcome (Fig. 4c). Furthermore, the hierarchical analysis of different clinical variables was performed on PRGscore. We first analyzed the distribution of PRGscore across levels of these clinical factors. As shown in Fig. S6a, PRGscore was significantly higher in patients with advanced cancer and recurrence than other patients. The PRGscore of patients receiving chemotherapy was also likely to be higher than that of patients receiving other treatments, although there was no statistical difference between the two. Patients with higher PRGscore were more likely to be in advanced stage, experiencing recurrence and receiving chemotherapy. Subsequently, through log-rank test, we found the PRGscore was significant associated with survival time in the smaller age, grade G3, stage III and IV and chemotherapy ($P < 0.05$, Fig. S6b).

After determining the prognostic value of PRGscore, we assessed the importance of PRGscore in immunology. First, we calculated the relevance of 22 immune cell types to the PRGscore with data from the CIBERSORT analysis and found that plasma cells, resting DCs, M1 macrophages, resting mast cells, neutrophils, γδ T cells, activated CD4 memory T cells and CD8 + T cells decreased with the increase of PRGscore, and the two were negatively correlated to a certain degree. In contrast, memory B cells, dendritic cells, activated mast cells, activated NK cells and resting CD4 + memory T cells had faint positive correlation with PRGscore (Fig. S7a). Subsequently, we evaluated the degree of tumor immune infiltration in high and low PRGscore groups with ssGSEA. Fig. 4D-E showed that apart from CD56dim NK cells and type 2 T helper cells, the infiltration of other immune cells was much greater in low PRGscore group than in high group and was negatively correlated with PRGscore ($P < 0.001$). Similarly, ESTIMATE algorithm results proved that there were more infiltrating mesenchymal and immune cells in tumor tissue in low PRGscore group, which also meant decreased in tumor purity ($P < 0.001$, Fig. 4f). GSEA revealed that the low PRGscore group could enrich several immune and matrix activation pathways, including BCR pathway and TCR pathway, chemokine signaling pathway and cytokine-cytokine receptor interaction signaling pathway. These studies also explained from the side why the low PRGscore group had a better prognosis (Fig. 4g).

3.5. Correlation between PRGscore and tumor burden mutation

The above results indirectly indicated that the difference in pyroptosis in tumors may be the key factor leading to different clinical responses of patients to immunotherapy. Research revealed a positive relation between TMB and tumor stage, grade and immune infiltrating cells [48]. Given the clinical importance of TMB, we sought to exploit the intrinsic connections that existed within TMB and PRGscore to elucidate the true markers of these two groups. First, we applied the maftools package to analyze the differences in the distribution of somatic mutations between low PRGscore and high PRGscore. As shown in Fig. 5A, the somatic mutation load in the two subgroups remained basically the same. TMB quantitative analysis confirmed that low PRGscore tumors were significantly correlated with higher TMB ($P = 0.022$, Fig. 5b). However, there was no statistical correlation between PRGscore and TMB (Fig. S7b).

Subsequently, we noticed that high TMB patients had superior overall survival (p = 0.016; Fig. 5c). Given the prognostic contraindications of TMB and PRGscore, we further explored the collaborative effectiveness of both scores in OC prediction stratification. Stratified analysis showed that TMB did not influence

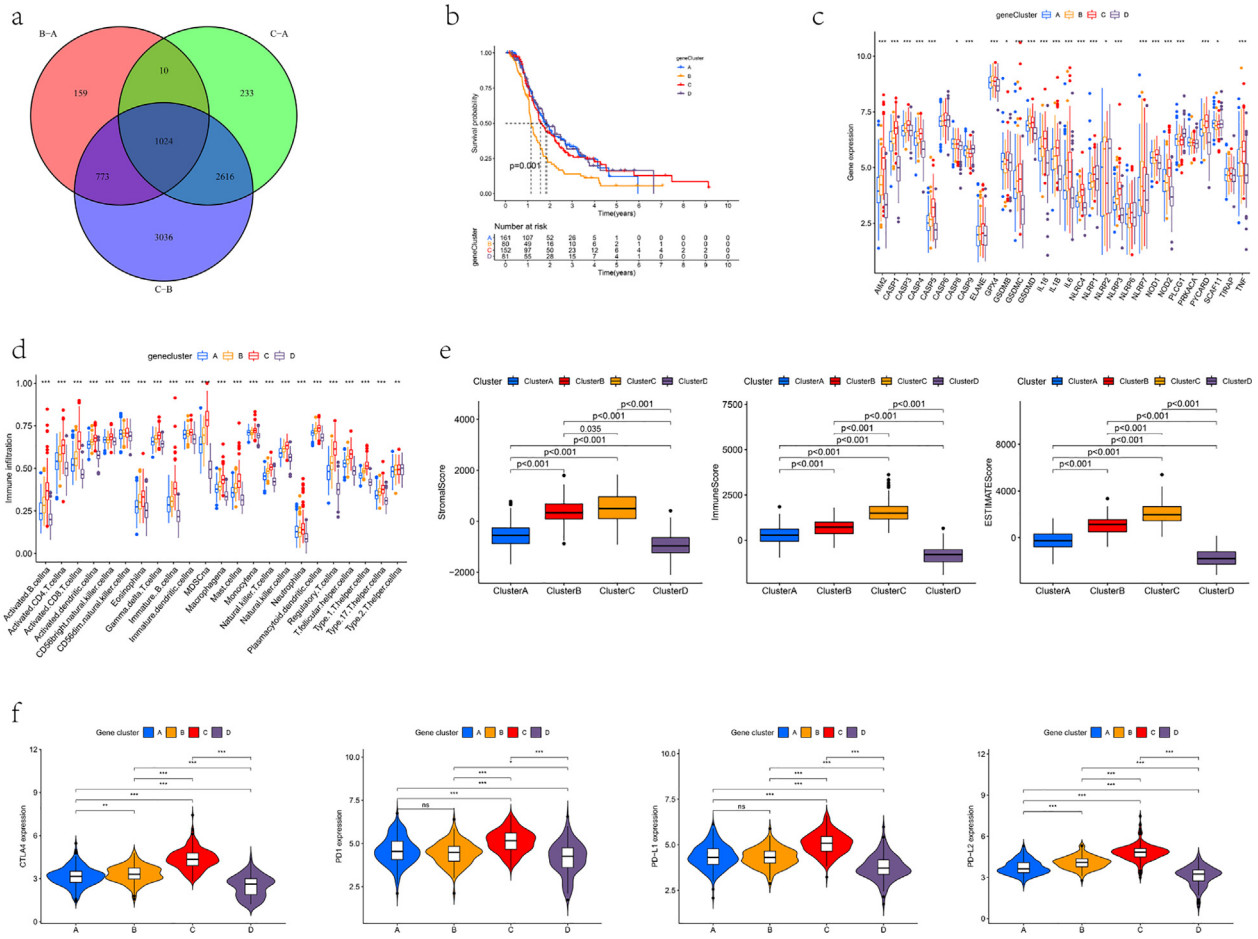

Fig. 3. Pyroptosis gene clusters and biological features of pyroptosis gene subgroupsa Venn plot performed different pyroptosis related genes between three PRGS clusters. b Kaplan-Meier curves shows pyroptosis gene types were correlated with overall survival of OC patients (P = 0.001, Log-rank test). c The expression of 30 PRGs in four gene clusters. d The abundance of each TME infiltrating cell. e The box plot shows difference in TME score between the gene clusters. f Difference of CTLA-4, PD1, PD-L1 and PD-L2 expression among four PRGs clusters.

prediction according to PRGscore, and PRGscore subtypes showed dramatic differences in prognosis among the two TMB subgroups (P = 0.015, Fig. 5d). For genes with specific changes in OC, such as MUC16 and TP53, the survival rate of the MUC16 mutant PRGscore group was noticeably poorer than that of wild type (P = 0.027, Fig. 5e), while the survival rate of the PRGscore group of the TP53 wild type was lower (P = 0.028, Fig. 5f). This also showed that the predictive ability of PRGscore was not interfered by gene mutations. Regardless of whether mutations occur or not, the high PRGscore group always showed poor overall survival (Fig. 5e and f)**.** The above results proved that PRGscore can be regarded as a predictor independent of tumor mutations. These results will offer novel perspectives on the mechanisms of tumor somatic mutation and pyroptosis in the TMB, and indirectly confirm the value of PRGscore in predicting the outcome of immunotherapy.

3.6. The role of pyroptosis pattern in the chemotherapy and immunotherapy treatment of OC

Currently, bleomycin plus etoposide plus cisplatin (BEP), paclitaxel plus platinum, and vinblastine, etc. are generally used as chemotherapy drugs for OC [49,50,51]. To this end, we explored whether the modified characteristics of pyroptosis can predict the patients' response to these chemotherapeutic drugs. As can be seen from Fig. 6a, high PRGscore group exhibited significant lower therapeutic sensitivity to the three drugs bleomycin, vinblastine and gemcitabine ($P \leq 0.0011$), while they were more sensitive to etoposide (P = 0.034). For cisplatin and paclitaxel, no statistical differences in drug sensitivity were observed between two groups (Fig. S7c). These conclusions were sufficient to show that PRGscore helped predict the patient's response to chemotherapy.

Then, we focused our analysis on the expression levels of immune checkpoints in high and low PRGscore subgroups and the correlation among them. Fig. 6b revealed that all immune checkpoint expression was much greater in low group versus high subgroup (P < 0.001) and that the immune checkpoints showed a highly significant negative correlation with PRGscore (P < 0.001, Fig. 6c). The immune checkpoint expression of health control group which marked as normal in Fig. 6b was different with OC patient groups. We also studied the expression of a number of immune molecules in PRGscore subgroups, such as *TNF, IFNG, CD8A* and *CXCL9*. Except for *TBX2,* other genes showing greater expression in low PRGscore group (Fig. 6d) might be vital in the higher survivability of low PRGscore group (Fig. 4c).

Subsequently, we used IPS scores to analyze the responsiveness of different subgroups to immunotherapy. IPS score is a determinant of tumor immunogenicity and can be used as an excellent predictor of anti-PD-1/CTLA-4 antibody response [42] which can separately evaluate the possibilities of patients receiving different ICIs treatments. From Fig. 6e, it can be seen that the score of the

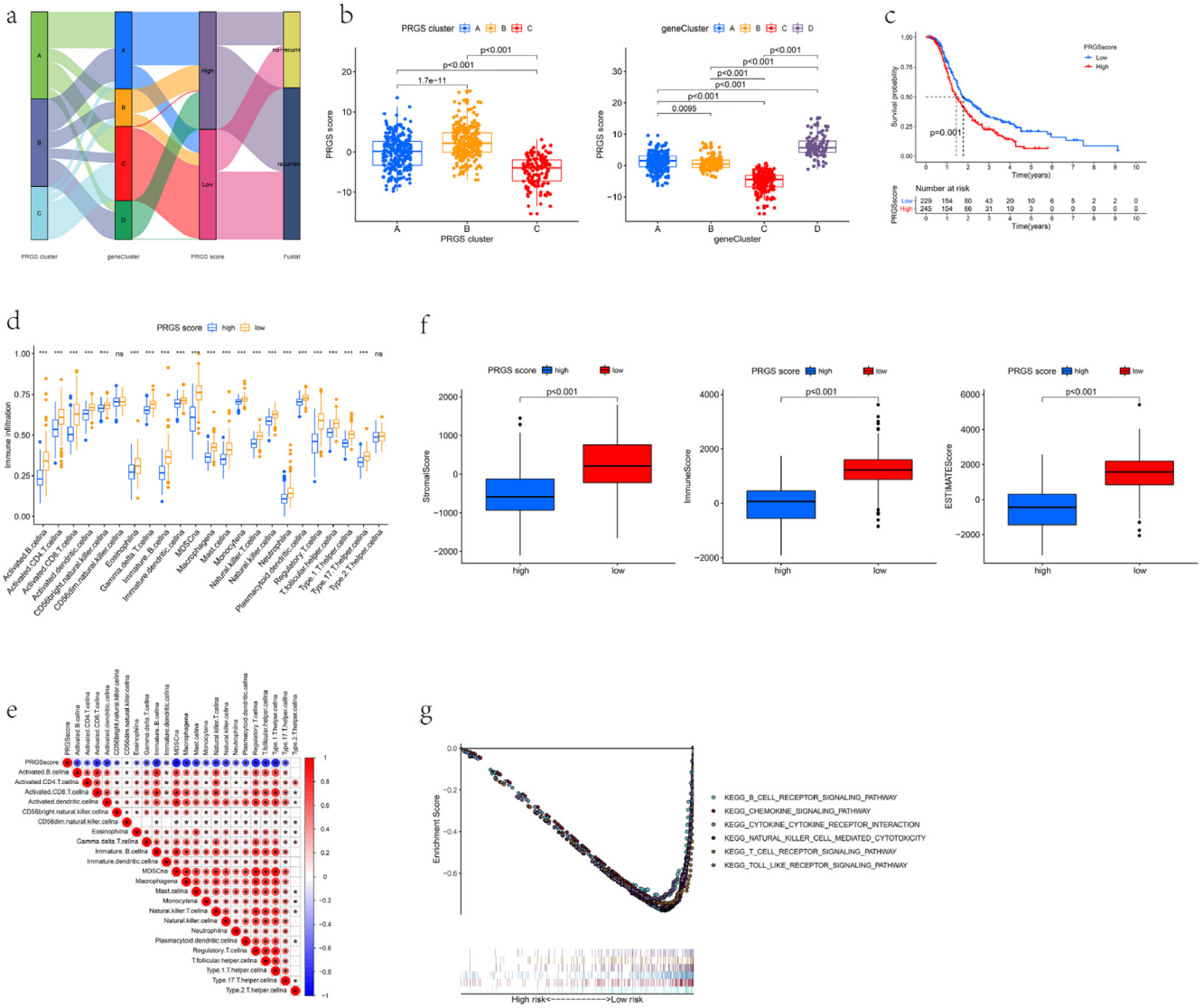

Fig. 4. Establishment of pyroptosis signaturesa Alluvial plot of the changes of PRclusters, gene cluster, PRGscore and survival status. b Distinctions in PRGscore among three PRclusters and four PRG gene cluster. The Kruskal Wallis test was applied to compare the statistical difference between the clusters ($P < 0.001$). c Survival analyses for low and high PRGscore patient groups in OC cohort. d The abundance of each infiltrating cell in PRGscore groups. e Correlations between PRGscore and immune cells. f The box plot showed difference in TME score between PRGscore subgroups. g Enrichment plots indicates that immune related pathway enriched in the low PRGscore subgroup.

low PRGscore group increased significantly ($P \leq 0.0043$). This indicated that the low PRGscore group showed higher IPS and appeared to have more immunogenic phenotypes. These results above implied that the quantification of pyroptosis may be applied as a hopeful and stable factor for the evaluation of chemotherapy response and immunotherapy.

3.7. Validation of PRGscore performance in predicting prognosis and immunotherapy response

New TCGA-UCEC and TCGA-CESC pyroptosis models and calculation of PRGscore utilizing the PCA analysis data of 67 genes acquired from the earlier analysis. Fig. 7a and b show the prognostic efficacy of PRGscore in predicting overall survival and disease-free survival (DFS) of CESC and UCEC, respectively. In CESC, low PRGscore likely caused favorable prognosis, which was in line with OC results. However, in UCSC, PRGscore cannot accurately predict patient survival. This indicated that pyroptosis was also likely to be involved in CESC development.

In addition, we further validated the relationship between PRGscore and immunotherapy efficacy using the imvigor210-BLCA cohort. First, as above, we calculated PRGscore in the imvigor210 cohort and divided the sample into high and low PRGscore group. Fig. 7c showed that the prognosis was significantly different among two groups, with low PRGscore group patients having a better prognosis. This also provided initial indications that low PRGscore patients who received immunotherapy had better outcomes than those with high PRGscore. Next, we analyzed the relationship between PRGscore and IC and TC immune types (Fig. 7d, e, f). At last, we analyzed the relationship between PRGscore, IC and TC immune types. We found that PRGscore was higher in IC0 than in IC1 and IC2, and PRGscore was higher in TC2 than in the other two groups, and PRGscore was higher in immune-desert type than in immune-inflamed and immune-excluded types ($P < 0.001$). These findings again suggested that PRGscore could be applied to predicting immunotherapy efficacy.

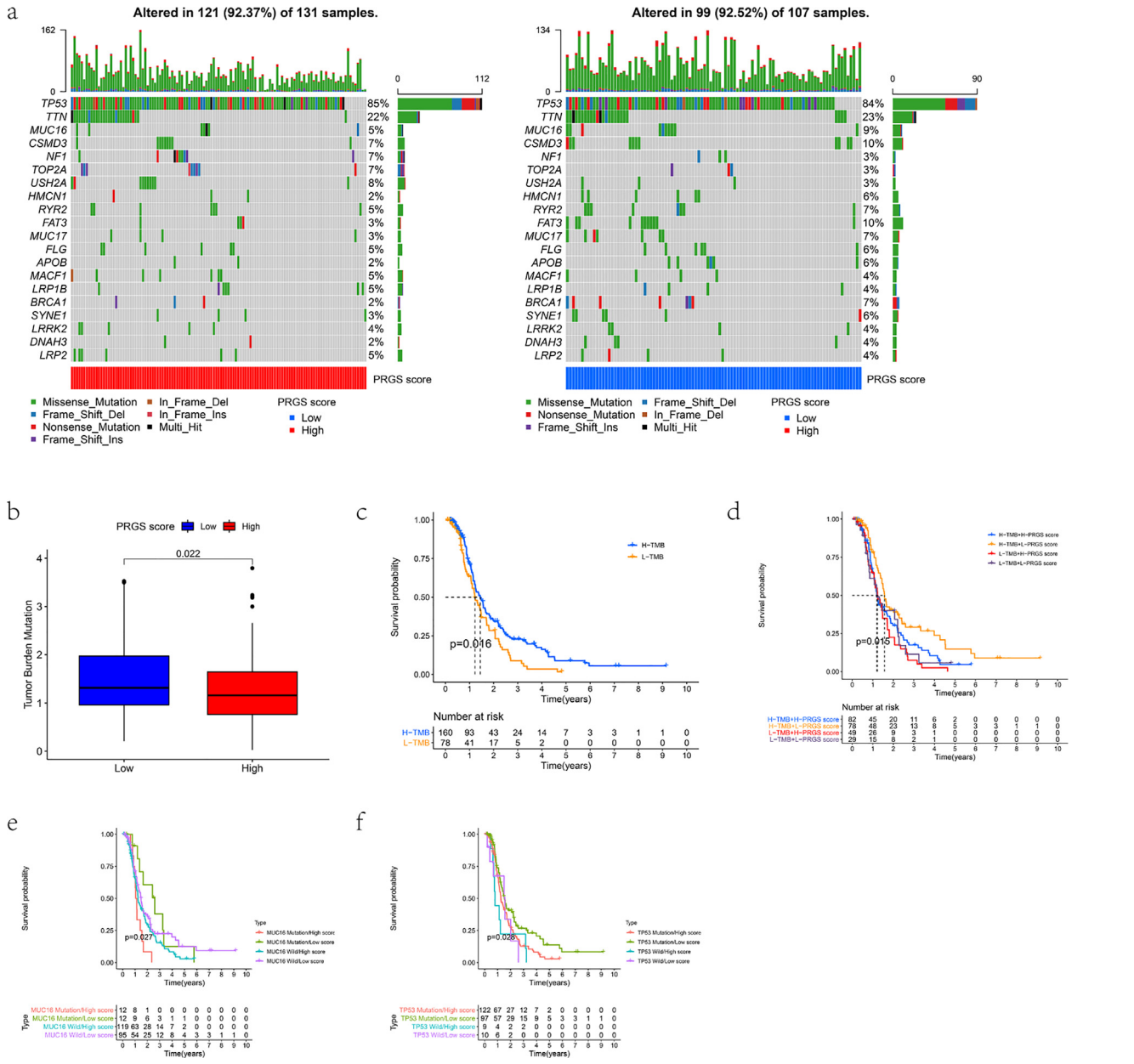

Fig. 5. The relationships between the PRGscore and Somatic Variantsa Mutation frequencies of PRGs in 131 and 107 patients with high and low PRGscore, respectively, from the TCGA cohort. b TMB difference in PRGscore subgroups. $P = 0.022$. c Kaplan-Meier curves for TMB groups, $P = 0.016$. d Kaplan-Meier curves for patients stratified by both TMB and PRGscores, $P = 0.015$. e Kaplan-Meier curves for patients stratified by both MUC16 and PRGscores, $P = 0.027$. f Kaplan-Meier curves for patients stratified by both TP53 and PRGscores, $P = 0.028$.

4. Discussion

Pyroptosis, an important immune response of the organism, is essential in combating infectious and pathogenic danger signals. It is broadly involved in the oncogenesis and progression of tumors, infection, metabolic diseases, neurological related disorders and atherosclerotic diseases [21,52,53]. Most of the previous studies focused on a single regulatory factor [54,55], so there is still a lack of a thorough knowledge of TME infiltration features mediated by multiple pyroptosis genes. Recently, studies have shown that pyroptosis can accurately predict the prognosis of OC [28]. In this work, we emphasized the contribution of pyroptosis in cell infiltration to improve the comprehension of anti-tumor immune, and tried to propose nichetargeting treatment options.

Based on 30 PRGs, we identified three different pyroptosis modification clusters which had different characteristics of TME cell infiltration. Combined with immune cell infiltration spectrum, we notice that cluster C is in consist with the immune-inflamed phenotype, which is marked by immune activation and massive immune cell infiltration. Cluster A belongs to immune-excluded type, which is marked by matrix activation and weakened immune infiltration. Although there is also massive immune cell infiltration in this type, most cells are in stroma surrounding the tumor cell nest, rather than penetrating parenchyma. This restricts immune cells from entering the tumor to be effective. The cluster B belongs to the immune-desert type which is correlated with immune resistance and absence of T cell activation [14]. The immune infection level of the healthy control group is significantly different from that of the case groups, which indicates that the patter is truly

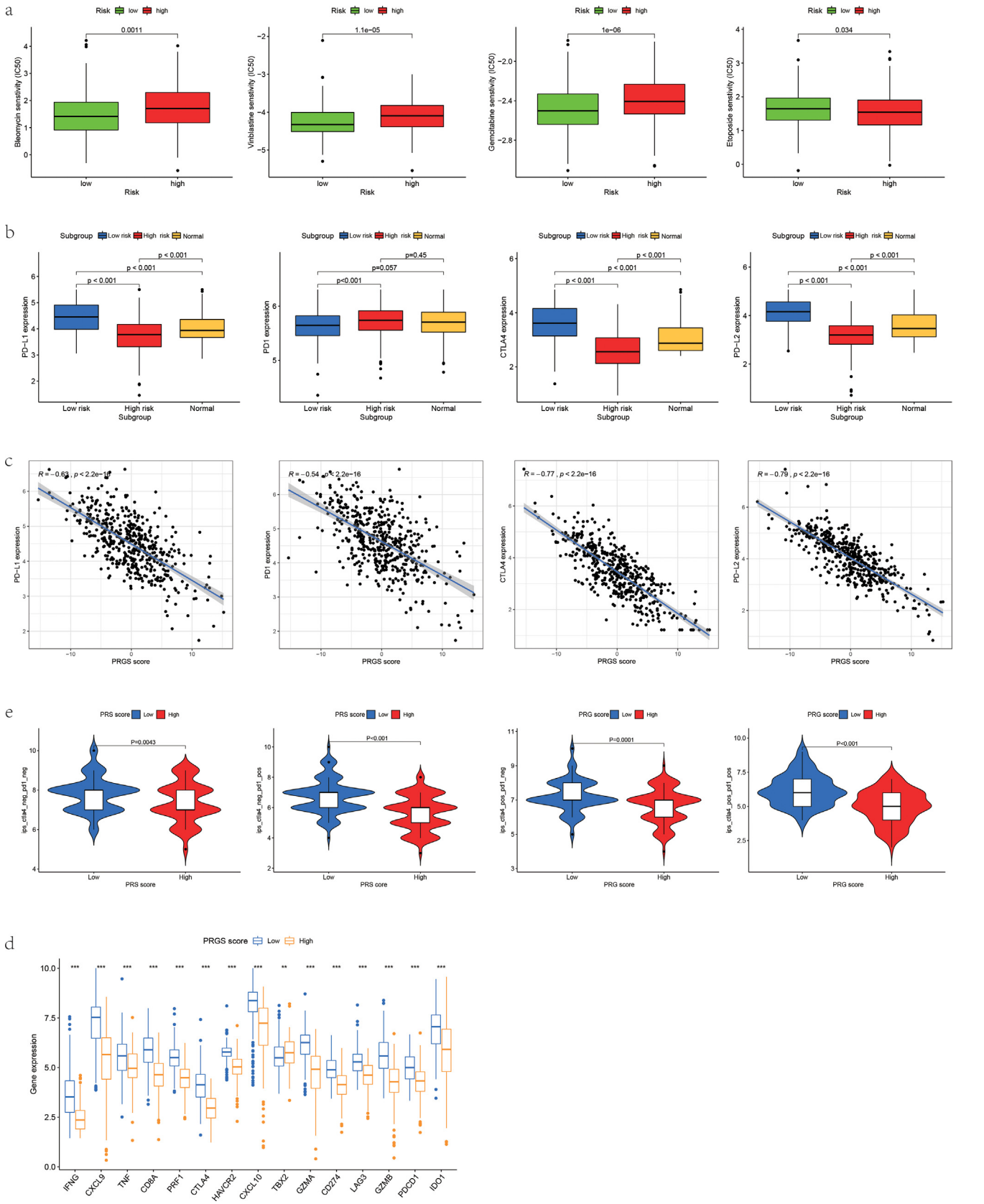

Fig. 6. Pyroptosis modification patterns in the therapy of OCa Box diagram indicating the sensitivity of patients to chemotherapy drugs,like bleomycin, vinblastine, gemcitabine and etoposide. b Different expression of CTLA-4, PD1, PD-L1 and PD-L2 among PRGscore subgroups together with normal group. c The correlations between PRGscore and immune checkpoints. d Immune-relevant genes expressed in PRGscore subgroups. e The difference of IPS between different PRGscore subgroups.

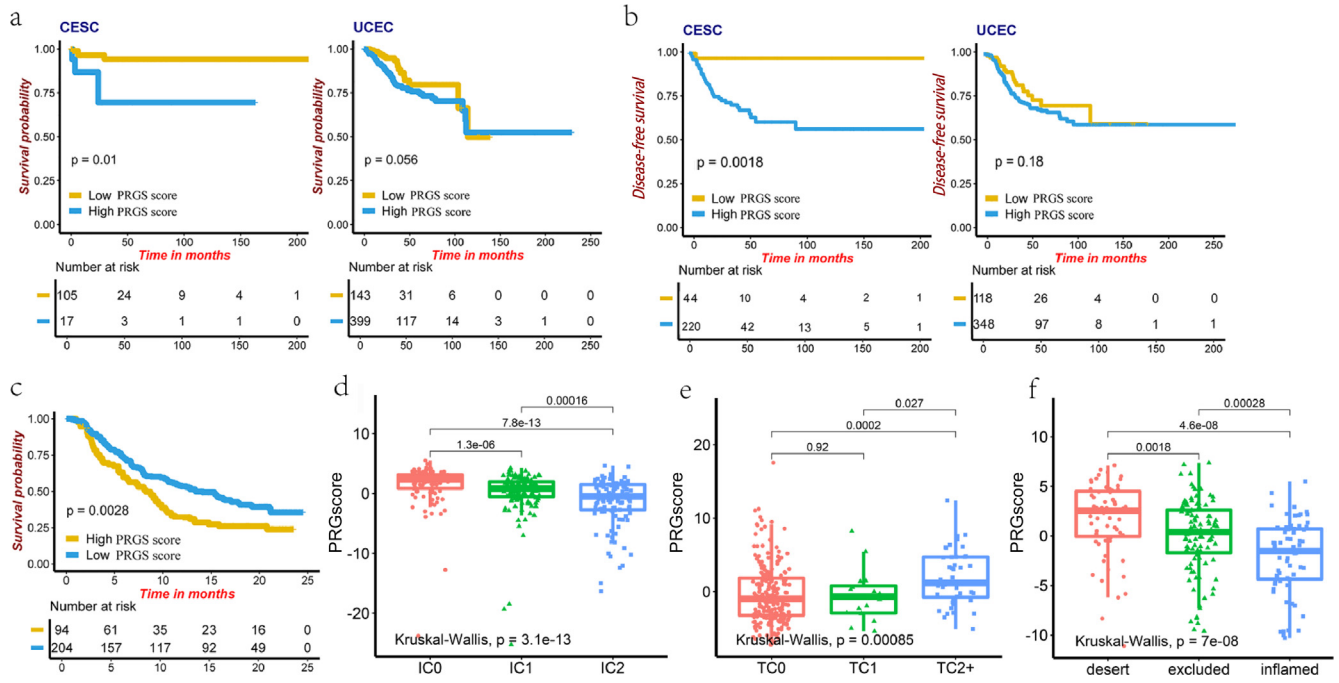

Fig. 7. Validation of prognostic performance of PRGscore in UCEC and CESCa Kaplan-Meier curves predict the overall survival rate of PRGcsore in CESC and UCEC patients. b Kaplan-Meier curves predict Disease Free Survival rate of PRGcsore in CESC and UCEC patients. c Kaplan–Meier plot of overall survival by PRGscore groups for patients in the IMvigor210 cohort. (d-e) The difference of PRGscore among PD-L1 expression of different IC (d) and TC (e) in the IMvigor210 cohort. Tumor tissue samples were scored through immunohistochemistry (IHC) for PDL1 expression on tumor-infiltrating immune cells (IC), which included macrophages, dendritic cells and lymphocytes. Specimens were scored as IHC IC0, IC1, IC2, or IC3 if < 1 %, ≥1% but < 5 %, ≥5% but < 10 %, or ≥ 10 % of IC were PD-L1 positive, respectively. An exploratory analysis of PD-L1 expression on tumor cells (TC) was conducted. Specimens were scored as IHC TC0, TC1, TC2, or TC3 if < 1 %, ≥1% but < 5 %, ≥5% but < 50 %, or ≥ 50 % of TC were PD-L1 positive, respectively. f Difference of PRGcsore among three immune subtypes.

working for patients but different from health controls. When combined with the characteristics of immune cell infiltration it not only proved the effectiveness of the immunophenotypic classification of pyroptosis modification patterns, but also helped to improve the future application of precise focusing and personalized treatment for OC. In addition, in this study, the genes that differ in the mRNA transcriptome among different pyroptosis modification patterns were considered to be characteristic pyroptosis related genes. Four gene clusters were identified based on differentially expressed genes which were related to matrix and immune activation. This illustrated the vital influence of pyroptosis modification on constructing a diverse TME landscape. An integrative analysis of the pattern of pyroptosis modifications could contribute to a further understanding of the characteristics of TME cell infiltration.

In view of the individual differences in pyroptosis modification, we applied a score system to evaluated pyroptosis modification condition of OC patients, called PRGscore. PRG cluster B showed the highest PRGscore and the worst clinical result, while PRG cluster C showed the opposite results. The results have also been proved in the pyroptosis gene cluster. This indicates that PRGscore is a reliable predictor for OC, and can be employed to evaluate tumor pyroptosis modification conditions.

Although immune checkpoint inhibitors have greatly improved the treatment and prognostic characteristics of many cancers, OC included [11], there are distinction in the effect of immunotherapy on patients. Therefore, looking for predictors that forecasting the outcome of immunotherapy has clinical significance. We confirm PRGscore predictive value in anti-PD-1/CTLA-4 immunotherapy cohorts, and found that patients with low PRGscore were more likely to receive ICI treatment. In addition, previous findings indicated that the existence of massive CD8 + T cell infiltrates and non-synonymous mutations promote response to anti-PD-1 therapy. We found a much higher degree of CD8 + T cell infiltration and TMB in low PRGscore group compared to high group, which also explained the good treatment effect of the low PRGscore group. Therefore, we proved that the pyroptosis modification mode played an important role in shaping different immune TME landscapes, which means that pyroptosis modification will affect the ICI treatment effect.

Chemotherapy is one of the primary treatments for OC [56]. The IC50 values of several commonly used chemotherapeutic drugs were measured and compared between the high- and low-risk subgroup, displaying that low PRGscore group exhibited significant therapeutic sensitivity to the three drugs bleomycin, vinblastine and gemcitabine, while patients in the high PRGscore group were more sensitive to etoposide. Therefore, the risk score could also be used to predict the effect of chemotherapeutic drugs on OC patients. Meanwhile, patients with high PRGscore had poor prognosis and poorImmunotherapeutic response. Combined therapy might be an effective treatment for OV patients, which needs further discussion. Doctors can choose the more effective treatment of every patient according to the PRGscore.

PRGscore was obtained by weighting some genes, a large part of which are immune checkpoints. The gene transcription level of IDO1 is closely related to T cell infiltration, and studies have shown that IDO1 expression is associated with poor prognosis in OC patients [57]. In addition to acting as a checkpoint of anti-cancer immunity, CD274 can be degraded through proteasome or lysosome through multiple pathways to enhanc the immunotherapeutic effect of cancer [58]. HAVCR2 is a key checkpoint molecule that regulates the inflammatory response which can induce T cell failure [59,60]. PDCD1 encodes cell surface facial mask proteins from the immunoglobulin superfamily, and its expression is related to a large number of tumor infiltrating lymphocytes in various tumors [61].CTLA4 is a target for monoclonal antibody-based drugs that

enhance anticancer immunity [62]. LAG3 is also an immunotherapeutic target, [63] it can inhibits the activation of its host cells and generally promotes inhibitory immune response [64]. CD8a + is mainly expressed on effector T cells. Previous studies have shown that drugs targeting immune populations may have pleiotropic effects on T cell dynamics and induce immune cells to enter tumors [65]. CXCL9, CXCL10 are involved in regulating immune cell migration, differentiation and activation, leading to tumor suppression [66]. IFNG mediates immune checkpoint expression, and interferon γ encoded by IFNG gene is one of the common cytokines known to affect immune related diseases [67]. TNF controls the development of the immune system, cell survival signaling pathways, proliferation, and regulates metabolic processes [68]. GZMA and GZMB belong to cytotoxic genes, and play important roles in cell death, cytokine processing and inflammation [69,70]. As a clear marker of the killing ability of immune cells, PRF1 is involved in the establishment of immune homeostasis, the elimination of pathogens and the monitoring of tumors [71]. BX2 is an anti-aging *T*-box family transcriptional repressor that has been implicated in embryonic development and cancer [72].

In clinical applications, PRGscore can be applied to evaluate individual patients' pyroptosis modification patterns and corresponding immune cell infiltration characteristics to promote the determination of immunophenotypes and direct effective medications. In addition, PRGscore can predict the effectiveness of adjuvant chemotherapy and immunotherapy. Therefore, we are here to provide clinicians with new ideas for immuno-oncology and OC individualized immunotherapy. However, our research has some limitations. Owing to the restricted availability of clinical annotation in public datasets, the clinical pathology variables detected in this work were not complete. When the PRGscore feature is used as a prognostic biomarker, there may be potential biases. Further clinical trials will be performed in future work to verify the outcomes.

5. Conclusion

In summary, this work examined the modifying effects of pyroptosis modification in the OC immune microenvironment and cell infiltration. Evaluating the modification pattern of pyroptosis in a single OC patient can help us fully understand the tumor immune condition and offer more effective treatments for OC patients.

6. Statements and Declarations

Contributors All authors contributed to the draft and have seen and approved the final version of the report.

Funding

This work was funded by the Jiangsu Province Nature Science Foundation (Grant No. BK20220729) and National Natural Science Foundation of China (Grant No. 82273738).

Declaration of Competing Interest

The authors declare that they have no known competing financial interests or personal relationships that could have appeared to influence the work reported in this paper.

Acknowledgement

The results shown here are in whole or part based upon data generated by TCGA, GEO database.

Appendix A. Supplementary data

Supplementary data to this article can be found online at https://doi.org/10.1016/j.csbj.2022.09.037.

References

[1] Stewart C, Ralyea C, Lockwood S. Ovarian Cancer: An Integrated Review. Semin Oncol Nurs 2019;35:151–6. https://doi.org/10.1016/j.soncn.2019.02.001.
[2] Colombo N, Van Gorp T, Parma G, Amant F, Gatta G, Sessa C, et al. Ovarian cancer. Crit Rev Oncol Hematol 2006;60:159–79. https://doi.org/10.1016/j.critrevonc.2006.03.004.
[3] Jessmon P, Boulanger T, Zhou W, Patwardhan P. Epidemiology and treatment patterns of epithelial ovarian cancer. Expert Rev Anticancer Ther 2017;17:427–37. https://doi.org/10.1080/14737140.2017.1299575.
[4] Narod S. Can advanced-stage ovarian cancer be cured? Nat Rev Clin Oncol 2016;13:255–61. https://doi.org/10.1038/nrclinonc.2015.224.
[5] Pujade-Lauraine E, Wagner U, Aavall-Lundqvist E, Gebski V, Heywood M, Vasey PA, et al. Pegylated liposomal Doxorubicin and Carboplatin compared with Paclitaxel and Carboplatin for patients with platinum-sensitive ovarian cancer in late relapse. J Clin Oncol 2010;28:3323–9. https://doi.org/10.1200/JCO.2009.25.7519.
[6] Behr M. Ovarian cancer. Medsurg Nurs 2009;18(248):252.
[7] Torre LA, Trabert B, DeSantis CE, Miller KD, Samimi G, Runowicz CD, et al. Ovarian cancer statistics, 2018. CA Cancer J Clin 2018;68:284–96. https://doi.org/10.3322/caac.21456.
[8] Rini BI, Plimack ER, Stus V, Gafanov R, Hawkins R, Nosov D, et al. Pembrolizumab plus Axitinib versus Sunitinib for Advanced Renal-Cell Carcinoma. N Engl J Med 2019;380:1116–27. https://doi.org/10.1056/NEJMoa1816714.
[9] Topalian SL, Hodi FS, Brahmer JR, Gettinger SN, Smith DC, McDermott DF, et al. Safety, activity, and immune correlates of anti-PD-1 antibody in cancer. N Engl J Med 2012;366:2443–54. https://doi.org/10.1056/NEJMoa1200690.
[10] Matulonis UA, Shapira-Frommer R, Santin AD, Lisyanskaya AS, Pignata S, Vergote I, et al. Antitumor activity and safety of pembrolizumab in patients with advanced recurrent ovarian cancer: results from the phase II KEYNOTE-100 study. Ann Oncol 2019;30:1080–7. https://doi.org/10.1093/annonc/mdz135.
[11] Hamanishi J, Mandai M, Ikeda T, Minami M, Kawaguchi A, Murayama T, et al. Safety and Antitumor Activity of Anti-PD-1 Antibody, Nivolumab, in Patients With Platinum-Resistant Ovarian Cancer. J Clin Oncol 2015;33:4015–22. https://doi.org/10.1200/JCO.2015.62.3397.
[12] Tse BW, Collins A, Oehler MK, Zippelius A, Heinzelmann-Schwarz VA. Antibody-based immunotherapy for ovarian cancer: where are we at? Ann Oncol 2014;25:322–31. https://doi.org/10.1093/annonc/mdt405.
[13] Binnewies M, Roberts EW, Kersten K, Chan V, Fearon DF, Merad M, et al. Understanding the tumor immune microenvironment (TIME) for effective therapy. Nat Med 2018;24:541–50. https://doi.org/10.1038/s41591-018-0014-x.
[14] Chen DS, Mellman I. Elements of cancer immunity and the cancer-immune set point. Nature 2017;541:321–30. https://doi.org/10.1038/nature21349.
[15] Hugo W, Zaretsky JM, Sun L, Song C, Moreno BH, Hu-Lieskovan S, et al. Genomic and Transcriptomic Features of Response to Anti-PD-1 Therapy in Metastatic Melanoma. Cell 2017;168:542. https://doi.org/10.1016/j.cell.2017.01.010.
[16] Kovacs SB, Miao EA. Gasdermins: Effectors of Pyroptosis. Trends Cell Biol 2017;27:673–84. https://doi.org/10.1016/j.tcb.2017.05.005.
[17] Shi J, Gao W, Shao F. Pyroptosis: Gasdermin-Mediated Programmed Necrotic Cell Death. Trends Biochem Sci 2017;42:245–54. https://doi.org/10.1016/j.tibs.2016.10.004.
[18] Xue Y, Enosi Tuipulotu D, Tan WH, Kay C, Man SM. Emerging Activators and Regulators of Inflammasomes and Pyroptosis. Trends Immunol 2019;40:1035–52. https://doi.org/10.1016/j.it.2019.09.005.
[19] Jorgensen I, Miao EA. Pyroptotic cell death defends against intracellular pathogens. Immunol Rev 2015;265:130–42. https://doi.org/10.1111/imr.12287.
[20] Liu X, Zhang Z, Ruan J, Pan Y, Magupalli VG, Wu H, et al. Inflammasome-activated gasdermin D causes pyroptosis by forming membrane pores. Nature 2016;535:153–8. https://doi.org/10.1038/nature18629.
[21] Bergsbaken T, Fink SL, Cookson BT. Pyroptosis: host cell death and inflammation. Nat Rev Microbiol 2009;7:99–109. https://doi.org/10.1038/nrmicro2070.
[22] Kolb R, Liu GH, Janowski AM, Sutterwala FS, Zhang W. Inflammasomes in cancer: a double-edged sword. Protein Cell 2014;5:12–20. https://doi.org/10.1007/s13238-013-0001-4.
[23] Coll RC, Robertson AA, Chae JJ, Higgins SC, Munoz-Planillo R, Inserra MC, et al. A small-molecule inhibitor of the NLRP3 inflammasome for the treatment of inflammatory diseases. Nat Med 2015;21:248–55. https://doi.org/10.1038/nm.3806.
[24] Jo EK, Kim JK, Shin DM, Sasakawa C. Molecular mechanisms regulating NLRP3 inflammasome activation. Cell Mol Immunol 2016;13:148–59. https://doi.org/10.1038/cmi.2015.95.

[25] Ding J, Wang K, Liu W, She Y, Sun Q, Shi J, et al. Erratum: Pore-forming activity and structural autoinhibition of the gasdermin family. Nature 2016;540:150. https://doi.org/10.1038/nature20106.
[26] Hou J, Zhao R, Xia W, Chang CW, You Y, Hsu JM, et al. PD-L1-mediated gasdermin C expression switches apoptosis to pyroptosis in cancer cells and facilitates tumour necrosis. Nat Cell Biol 2020;22:1264–75. https://doi.org/10.1038/s41556-020-0575-z.
[27] Kiss M, Vande Walle L, Saavedra PHV, Lebegge E, Van Damme H, Murgaski A, et al. IL1beta Promotes Immune Suppression in the Tumor Microenvironment Independent of the Inflammasome and Gasdermin D. Cancer Immunol Res 2021;9:309–23. https://doi.org/10.1158/2326-6066.CIR-20-0431.
[28] Ye Y, Dai Q, Qi H. A novel defined pyroptosis-related gene signature for predicting the prognosis of ovarian cancer. Cell Death Discov 2021;7:71. https://doi.org/10.1038/s41420-021-00451-x.
[29] Cancer Genome Atlas Research N (2011) Integrated genomic analyses of ovarian carcinoma. Nature 474, 609-615, doi: 10.1038/nature10166.
[30] Consortium GT (2015) Human genomics. The Genotype-Tissue Expression (GTEx) pilot analysis: multitissue gene regulation in humans. Science 348, 648-660, doi: 10.1126/science.1262110.
[31] Edgar R, Domrachev M, Lash AE. Gene Expression Omnibus: NCBI gene expression and hybridization array data repository. Nucleic Acids Res 2002;30:207–10. https://doi.org/10.1093/nar/30.1.207.
[32] Mounir M, Lucchetta M, Silva TC, Olsen C, Bontempi G, Chen X, et al. New functionalities in the TCGAbiolinks package for the study and integration of cancer data from GDC and GTEx. PLoS Comput Biol 2019;15:e1006701.
[33] Ritchie ME, Phipson B, Wu D, Hu Y, Law CW, Shi W, et al. limma powers differential expression analyses for RNA-sequencing and microarray studies. Nucleic Acids Res 2015;43:e47.
[34] Tothill RW, Tinker AV, George J, Brown R, Fox SB, Lade S, et al. Novel molecular subtypes of serous and endometrioid ovarian cancer linked to clinical outcome. Clin Cancer Res 2008;14:5198–208. https://doi.org/10.1158/1078-0432.CCR-08-0196.
[35] Love MI, Huber W, Anders S. Moderated estimation of fold change and dispersion for RNA-seq data with DESeq2. Genome Biol 2014;15:550. https://doi.org/10.1186/s13059-014-0550-8.
[36] Mayakonda A, Lin DC, Assenov Y, Plass C, Koeffler HP. Maftools: efficient and comprehensive analysis of somatic variants in cancer. Genome Res 2018;28:1747–56. https://doi.org/10.1101/gr.239244.118.
[37] Wilkerson MD, Hayes DN. ConsensusClusterPlus: a class discovery tool with confidence assessments and item tracking. Bioinformatics 2010;26:1572–3. https://doi.org/10.1093/bioinformatics/btq170.
[38] Hanzelmann S, Castelo R, Guinney J. GSVA: gene set variation analysis for microarray and RNA-seq data. BMC Bioinf 2013;14:7. https://doi.org/10.1186/1471-2105-14-7.
[39] Yu G, Wang LG, Han Y, He QY. clusterProfiler: an R package for comparing biological themes among gene clusters. OMICS 2012;16:284–7. https://doi.org/10.1089/omi.2011.0118.
[40] Barbie DA, Tamayo P, Boehm JS, Kim SY, Moody SE, Dunn IF, et al. Systematic RNA interference reveals that oncogenic KRAS-driven cancers require TBK1. Nature 2009;462:108–12. https://doi.org/10.1038/nature08460.
[41] Sotiriou C, Wirapati P, Loi S, Harris A, Fox S, Smeds J, et al. Gene expression profiling in breast cancer: understanding the molecular basis of histologic grade to improve prognosis. J Natl Cancer Inst 2006;98:262–72. https://doi.org/10.1093/jnci/djj052.
[42] Charoentong P, Finotello F, Angelova M, Mayer C, Efremova M, Rieder D, et al. Pan-cancer Immunogenomic Analyses Reveal Genotype-Immunophenotype Relationships and Predictors of Response to Checkpoint Blockade. Cell Rep 2017;18:248–62. https://doi.org/10.1016/j.celrep.2016.12.019.
[43] Yoshihara K, Shahmoradgoli M, Martinez E, Vegesna R, Kim H, Torres-Garcia W, et al. Inferring tumour purity and stromal and immune cell admixture from expression data. Nat Commun 2013;4:2612. https://doi.org/10.1038/ncomms3612.
[44] Yang W, Soares J, Greninger P, Edelman EJ, Lightfoot H, Forbes S, Bindal N, Beare D, Smith JA, Thompson IR, Ramaswamy S, Futreal PA, Haber DA, Stratton MR, Benes C, McDermott U & Garnett MJ (2013) Genomics of Drug Sensitivity in Cancer (GDSC): a resource for therapeutic biomarker discovery in cancer cells. *Nucleic Acids Res* 41, D955-961, doi: 10.1093/nar/gks1111.
[45] Geeleher P, Cox NJ, Huang RS. Clinical drug response can be predicted using baseline gene expression levels and in vitro drug sensitivity in cell lines. Genome Biol 2014;15:R47. https://doi.org/10.1186/gb-2014-15-3-r47.
[46] Mariathasan S, Turley SJ, Nickles D, Castiglioni A, Yuen K, Wang Y, et al. TGFbeta attenuates tumour response to PD-L1 blockade by contributing to exclusion of T cells. Nature 2018;554:544–8. https://doi.org/10.1038/nature25501.
[47] Zhang H, Meltzer P, Davis S. RCircos: an R package for Circos 2D track plots. BMC Bioinf 2013;14:244. https://doi.org/10.1186/1471-2105-14-244.
[48] Bi F, Chen Y, Yang Q. Significance of tumor mutation burden combined with immune infiltrates in the progression and prognosis of ovarian cancer. Cancer Cell Int 2020;20:373. https://doi.org/10.1186/s12935-020-01472-9.
[49] Armstrong DK, Bundy B, Wenzel L, Huang HQ, Baergen R, Lele S, et al. Intraperitoneal cisplatin and paclitaxel in ovarian cancer. N Engl J Med 2006;354:34–43. https://doi.org/10.1056/NEJMoa052985.
[50] Williams S, Blessing JA, Liao SY, Ball H, Hanjani P. Adjuvant therapy of ovarian germ cell tumors with cisplatin, etoposide, and bleomycin: a trial of the Gynecologic Oncology Group. J Clin Oncol 1994;12:701–6. https://doi.org/10.1200/JCO.1994.12.4.701.
[51] Lyseng-Williamson KA, Duggan ST, Keating GM. Pegylated liposomal doxorubicin: a guide to its use in various malignancies. BioDrugs 2013;27:533–40. https://doi.org/10.1007/s40259-013-0070-1.
[52] Kesavardhana S, Malireddi RKS, Kanneganti TD. Caspases in Cell Death, Inflammation, and Pyroptosis. Annu Rev Immunol 2020;38:567–95. https://doi.org/10.1146/annurev-immunol-073119-095439.
[53] Man SM, Karki R, Kanneganti TD. Molecular mechanisms and functions of pyroptosis, inflammatory caspases and inflammasomes in infectious diseases. Immunol Rev 2017;277:61–75. https://doi.org/10.1111/imr.12534.
[54] Yu J, Li S, Qi J, Chen Z, Wu Y, Guo J, et al. Cleavage of GSDME by caspase-3 determines lobaplatin-induced pyroptosis in colon cancer cells. Cell Death Dis 2019;10:193. https://doi.org/10.1038/s41419-019-1441-4.
[55] Shen X, Wang H, Weng C, Jiang H, Chen J. Caspase 3/GSDME-dependent pyroptosis contributes to chemotherapy drug-induced nephrotoxicity. Cell Death Dis 2021;12:186. https://doi.org/10.1038/s41419-021-03458-5.
[56] Yang C, Xia BR, Zhang ZC, Zhang YJ, Lou G, Jin WL. Immunotherapy for Ovarian Cancer: Adjuvant, Combination, and Neoadjuvant. Front Immunol 2020;11:. https://doi.org/10.3389/fimmu.2020.577869577869.
[57] Zhai L, Ladomersky E, Lenzen A, Nguyen B, Patel R, Lauing KL, et al. IDO1 in cancer: a Gemini of immune checkpoints. Cell Mol Immunol 2018;15:447–57. https://doi.org/10.1038/cmi.2017.143.
[58] Gou Q, Dong C, Xu H, Khan B, Jin J, Liu Q, et al. PD-L1 degradation pathway and immunotherapy for cancer. Cell Death Dis 2020;11:955. https://doi.org/10.1038/s41419-020-03140-2.
[59] Huang YH, Zhu C, Kondo Y, Anderson AC, Gandhi A, Russell A, et al. CEACAM1 regulates TIM-3-mediated tolerance and exhaustion. Nature 2015;517:386–90. https://doi.org/10.1038/nature13848.
[60] Koh J, Jang I, Mun S, Lee C, Cha HJ, Oh YH, et al. Genetic profiles of subcutaneous panniculitis-like T-cell lymphoma and clinicopathological impact of HAVCR2 mutations. Blood Adv 2021;5:3919–30. https://doi.org/10.1182/bloodadvances.2021004562.
[61] Miao Y, Wang J, Li Q, Quan W, Wang Y, Li C, et al. Prognostic value and immunological role of PDCD1 gene in pan-cancer. Int Immunopharmacol 2020;89:. https://doi.org/10.1016/j.intimp.2020.107080107080.
[62] Liu JN, Kong XS, Huang T, Wang R, Li W, Chen QF. Clinical Implications of Aberrant PD-1 and CTLA4 Expression for Cancer Immunity and Prognosis: A Pan-Cancer Study. Front Immunol 2020;11:2048. https://doi.org/10.3389/fimmu.2020.02048.
[63] Andrews LP, Marciscano AE, Drake CG, Vignali DA. LAG3 (CD223) as a cancer immunotherapy target. Immunol Rev 2017;276:80–96. https://doi.org/10.1111/imr.12519.
[64] Graydon CG, Mohideen S, Fowke KR. LAG3's Enigmatic Mechanism of Action. Front Immunol 2020;11:. https://doi.org/10.3389/fimmu.2020.615317615317.
[65] Kristensen LK, Frohlich C, Christensen C, Melander MC, Poulsen TT, Galler GR, et al. CD4(+) and CD8a(+) PET imaging predicts response to novel PD-1 checkpoint inhibitor: studies of Sym021 in syngeneic mouse cancer models. Theranostics 2019;9:8221–38. https://doi.org/10.7150/thno.37513.
[66] Tokunaga R, Zhang W, Naseem M, Puccini A, Berger MD, Soni S, et al. CXCL9, CXCL10, CXCL11/CXCR3 axis for immune activation - A target for novel cancer therapy. Cancer Treat Rev 2018;63:40–7. https://doi.org/10.1016/j.ctrv.2017.11.007.
[67] Huang J, Chen P, Liu K, Liu J, Zhou B, Wu R, et al. CDK1/2/5 inhibition overcomes IFNG-mediated adaptive immune resistance in pancreatic cancer. Gut 2021;70:890–9. https://doi.org/10.1136/gutjnl-2019-320441.
[68] Varfolomeev E, Vucic D. Intracellular regulation of TNF activity in health and disease. Cytokine 2018;101:26–32. https://doi.org/10.1016/j.cyto.2016.08.035.
[69] Cheng Q, Chen X, Wu H, Du Y. Three hematologic/immune system-specific expressed genes are considered as the potential biomarkers for the diagnosis of early rheumatoid arthritis through bioinformatics analysis. J Transl Med 2021;19:18. https://doi.org/10.1186/s12967-020-02689-y.
[70] Zhou S, Lu H, Xiong M. Identifying Immune Cell Infiltration and Effective Diagnostic Biomarkers in Rheumatoid Arthritis by Bioinformatics Analysis. Front Immunol 2021;12:. https://doi.org/10.3389/fimmu.2021.726747726747.
[71] Fan C, Hu H, Shen Y, Wang Q, Mao Y, Ye B, et al. PRF1 is a prognostic marker and correlated with immune infiltration in head and neck squamous cell carcinoma. Transl Oncol 2021;14:. https://doi.org/10.1016/j.tranon.2021.101042101042.
[72] Lu S, Louphrasitthiphol P, Goradia N, Lambert JP, Schmidt J, Chauhan J, et al. TBX2 controls a proproliferative gene expression program in melanoma. Genes Dev 2021;35:1657–77. https://doi.org/10.1101/gad.348746.121.